

MICROSCOPIC STUDY OF ANGULAR MOMENTUM UNFAVORED  $O^+$  CHANNELS  
FOR THE  $^{16}O - ^{16}O$  AND  $\alpha - ^{16}O$  SYSTEMS

H.P. Brall, R. Stademann, K. Langanke and A. Weiguny  
Institut für Theoretische Physik  
Universität Münster, D-4400 Münster

The study of coupling of elastic and inelastic  $O^+$  channels is of special interest, because standard (phenomenological) models like the double resonance mechanism or the band crossing model<sup>1</sup> do not predict strong correlations between such channels. On the other hand, definite experimental evidence<sup>2</sup> exists for strong correlations between the  $^{16}O - ^{16}O$  elastic and  $^{16}O - ^{16}O(O_2^+)$  inelastic channels. In the present contribution, the problem of angular momentum unfavored channels is studied on a microscopic level within the framework of the generator coordinate method; the above  $^{16}O - ^{16}O$  case as well as the  $\alpha - ^{16}O$  system serve as specific examples. Using the Kohn-Hulthen variational principle, the coupled channel equations are solved with scattering boundary conditions; as a result, the full  $2 \times 2$  S-matrix is obtained.

Using Brink's alpha cluster model<sup>3</sup> the ground state wave function of  $^{16}O$  is associated with a regular tetrahedron of cluster centers, whereas the intrinsic configuration of the second  $O^+$  state in  $^{16}O$  is approximated by a planar rhomb. With the B1 force and oscillator width of  $b=1.604$  fm (corresponding to rms radii of 2.42 fm and 3.22 fm, resp.) the excitation energy is 6.05 MeV in agreement with experiment. The energy surfaces (Fig.1) support the sketch of the different behaviour of the two channels in ref. 4, based on the internal symmetry of the fragments and the Pauli principle.

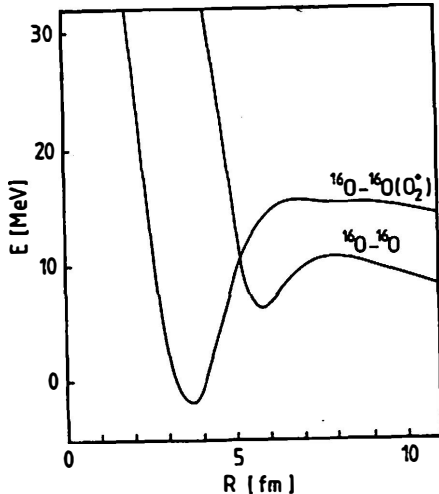


Fig.1 Energy surfaces for  $\ell=0$  for above  $^{16}O$  channels

Fig. 2 shows the resonance positions and widths obtained from the diagonal phase shifts. In contrast to the  $^{16}O - ^{16}O$  system which shows only one molecular band with a bandhead at  $E_0 = 7.98$  MeV and a rotational constant of 66.4 keV one gets two bands for the  $^{16}O - ^{16}O(O_2^+)$  system (-4.62 MeV, 107.0 keV; 6.18 MeV, 87.9 keV). For  $\ell=12$  the very sharp ( $\Gamma=1eV$ ) resonance of the lower  $^{16}O - ^{16}O(O_2^+)$  band lies within the width of the  $^{16}O - ^{16}O$  resonance. Fig.3 shows the correspondence between the maximum of the reaction flux  $|S_{12}|^2$  and the  $\ell=12$  diagonal phase shifts.

In contrast to the assumptions of phenomenological band crossing models, the present calculation indicates that the band structures in the elastic and inelastic channels are quite different, partly because of weaker Pauli repulsion in the inelastic channel<sup>5</sup>. The resulting band coexistence opens<sup>6</sup> the possibility for rotational band crossing even in the case

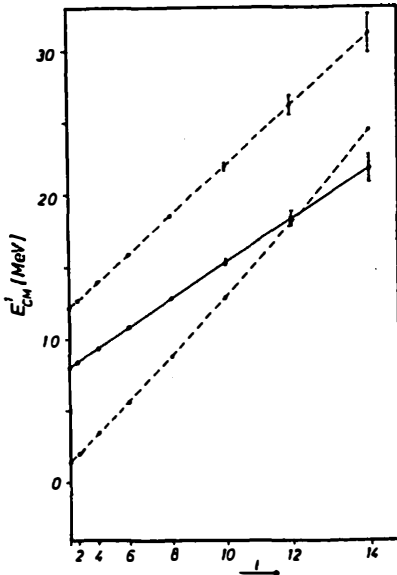


Fig. 2. Rotational bands of the  $^{16}\text{O} - ^{16}\text{O}$  (solid line) and  $^{16}\text{O} - ^{16}\text{O}(\text{O}_2^+)$  system (dashed line)

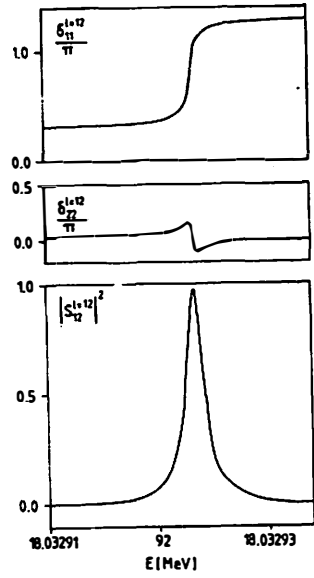


Fig. 3. Diagonal phase shifts and  $|S_{1,2}|^2$  for partial wave  $l=12$ .

of an intrinsic  $\text{O}^+$  excitation. The channel coupling turns out too weak to shift the unperturbed resonances noticeably. Hence the present study does not support the (phenomenological) strong coupling model of Mosel and Tanimura<sup>7</sup> assuming equal diagonal potentials for both channels. Compared to experiment<sup>2</sup>, the inelastic cross section is (on average) about 2 orders of magnitude too small and shows too little structure. Taking into account distortion of the  $^{16}\text{O}(\text{O}_2)$  fragment by admixing bent rhombic configurations (which have larger overlap with the tetrahedron of the  $^{16}\text{O}$  intrinsic ground state), the cross section increases by 1 order of magnitude. Further configurations and/or an improved effective force (on which the band structure depends!) will be necessary to reach experiment.

The situation is quite different for the  $\alpha - ^{18}\text{O}$  system where the Pauli forbidden states are the same for both channels in contrast to the  $^{16}\text{O} - ^{16}\text{O}$  system<sup>6</sup>. Diagonalizing the internal  $^{18}\text{O}$  Hamiltonian with the Volkov V1 force in the space of functions

$$\Phi_1 \hat{=} \mathcal{A} \{ (\text{Os})^4 (\text{Op})^{12} [(\text{Od}_{5/2})^2]_{J=0} \}$$

$$\bar{\phi}_2 \hat{=} \mathcal{A} \{ (Os)^4 (Op)^{12} [(1s_{1/2})^2]_{J=0} \}$$

one obtains, with the Volkov V1 force and an oscillator width of  $b = 1.49$  fm,

and  $\phi_1 = 0.873 \bar{\phi}_1 + 0.487 \bar{\phi}_2$  for the ground state

$\phi_2 = 0.487 \bar{\phi}_1 - 0.873 \bar{\phi}_2$  for the  $O_2^+$  excited state.

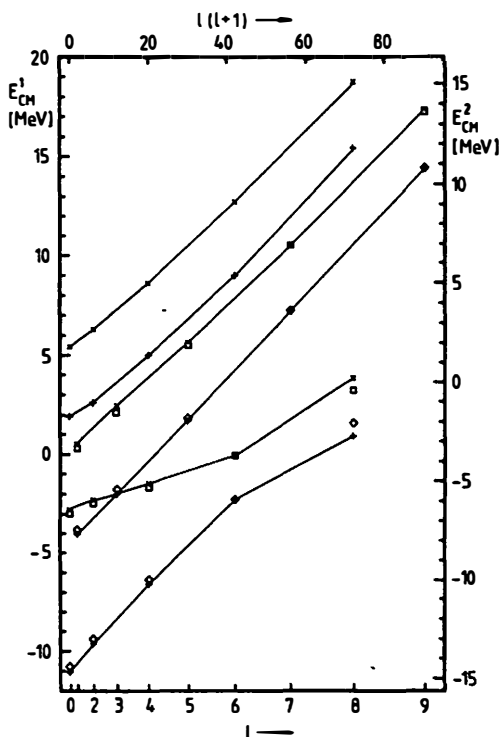


Fig. 4. Rotational bands of elastic (+,  $\diamond$ ) and inelastic channel (x,  $\square$ ) with and without channel coupling, resp.

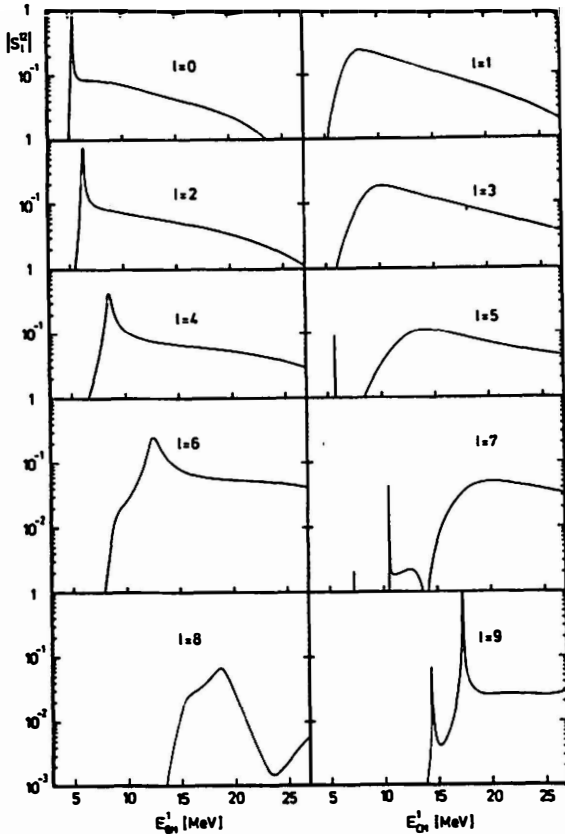
band structure of the elastic channel, in accordance with the assumption of the band crossing model.

But although the rotational bands do not cross, the reaction flux (Fig. 5) is strongly enhanced in the vicinity of inelastic channel barrier resonances for positive parity. The corresponding maxima for negative parity are broad and comparatively weak, except for  $\ell=9$  where the inelastic molecular resonance at 17.3 MeV lies within the width of the elastic barrier resonance.  $|S_{12}|$  reaches 0.986 in this case as expected from the double

The excitation energy has been adjusted from its theoretical value of 2.6 MeV to the experimental one of 3.63 MeV in the coupled channel calculation. The channel wave functions are defined via the anti-symmetrized products of the  $(Os)^4$ -state for the  $\alpha$ -particle with  $\phi_1$  and  $\phi_2$ , resp.

Fig. 4 shows the resonance positions of the coupled and decoupled channels. In contrast to the  $^{16}O$ - $^{16}O$ -system, the band structures in the elastic and inelastic channels are quite similar. Only the ground state bands whose members show up a shell model like character differ in their rotational constants. The influence of the internal  $^{16}O$ -structure on the negative parity and excited positive parity cluster-like states is small. In the inelastic channel the corresponding rotational bands are shifted by about the threshold energy of 3.63 MeV compared to the

resonance mechanism. Since the change in configuration is restricted to only two nucleons, the channel coupling is on average much stronger than in the case of the  $^{16}\text{O}-^{16}\text{O}$  channels. Nevertheless, the unperturbed resonances are only weakly shifted and the channel mixing is less than 5%, except for the lower  $8^+$ -states (21.5%), where the bands come close to each other.



A very important point not taken into account by phenomenological models is a strong  $l$ -dependence of the channel coupling resulting from the Pauli-principle. This  $l$ -dependence becomes visible in the irregular behavior of the inelastic channel relative partial widths ( $\Gamma_2/\Gamma$ )  $\approx 0.002$ ,  $0.9996$  and  $0.583$  of the  $5^-$ ,  $7^-$  and  $9^-$  inelastic molecular resonances, resp., pointing out a rather weak channel coupling in partial wave  $l=7$  compared to  $l=5$ ,  $9$ . Due to the smaller barrier penetrability, the peaks resulting from the  $7^-$  and  $9^-$  elastic molecular resonances are reduced by more than one order of magnitude compared to those of the inelastic molecular resonances.

Fig.5. Absolute value of the partial wave S-matrix element  $S_l^{12}$  for  $\alpha-^{16}\text{O}$ .

1. Y. Abe, Y. Kondo and T. Matsuse, Prog. Theor. Phys. Suppl. No. 68 (1980); W. Scheid, W. Greiner and W. Lemmer, Phys. Rev. Lett. 25 (1970) 176
2. P. Paul et al., Phys. Rev. Lett. 45 (1981) 1479
3. D. M. Brink, Proc. Internat. School of Physics, Course 36 (1965) 247
4. M. Harvey, Proc. Intern. Conf. on Clustering Phenomena in Nuclei, College Park, Maryland (1975)
5. D. Wintgen et al., Nucl. Phys. A 402 (1983) 40
6. K. Langanke, H. Friedrich and S. E. Koonin, Phys. Rev. Letters 51 (1983) 1231
7. U. Mosel and O. Tanimura, Phys. Rev. C 24 (1981) 321